



WO₃-based catalysts prepared by non-hydrolytic sol-gel for the production of propene by cross-metathesis of ethene and 2-butene

Surasa Maksasithorn^a, Piyasan Praserthdam^a, Kongkiat Suriye^b, Michel Devillers^c,
Damien P. Debecker^{c,*}

^a Center of Excellence on Catalysis and Catalytic Reaction Engineering, Department of Chemical Engineering, Faculty of Engineering, Chulalongkorn University, Bangkok 10330, Thailand

^b SCG Chemicals, Co., Ltd., 1 Siam Cement Road, Bangsue, Bangkok 10800, Thailand

^c Institute of Condensed Matter and Nanoscience—Molecules, Solids and Reactivity (IMCN/MOST), Université catholique de Louvain, Croix du Sud 2/17, 1348 Louvain-La-Neuve, Belgium



ARTICLE INFO

Article history:

Received 15 August 2014

Received in revised form

17 September 2014

Accepted 21 September 2014

Available online 28 September 2014

Keywords:

Propylene

WO₃/SiO₂ catalyst

Non hydrolytic sol-gel

Non-aqueous sol-gel

Mesoporous mixed oxides

ABSTRACT

One-step non-hydrolytic sol-gel (NHSG) route is presented as a powerful method to prepare highly effective alkene metathesis catalysts. Tungsten-based catalysts are the industrially relevant system and are prepared for the first time using NHSG. The catalysts were characterized by N₂-physisorption, XRD, NH₃-TPD, NH₃-chemisorption, XPS, TPR, ICP-AES and evaluated in the cross-metathesis of ethene and *trans*-2-butene to propene. These new catalysts are systematically compared with reference catalysts prepared by impregnation methods on 2 commercial supports (silica and silica-alumina). NHSG catalysts markedly outcompete reference impregnated catalysts in terms of conversion, selectivity and stability. Characterization results show that the texture, tungsten dispersion, reducibility and surface acidity of the NHSG catalysts depend strongly on their composition. This in turn can be correlated with the catalytic performance.

© 2014 Elsevier B.V. All rights reserved.

1. Introduction

Propene is a major bulk chemical for the industry, as it is used as raw material for a wide variety of products such as polypropylene, acrylonitrile, propene oxide, etc. The majority of propene is obtained from steam crackers and fluid catalytic cracking units as a co-product and it is also produced marginally via propane dehydrogenation and methanol to olefin conversion [1]. Because propene demand is forecasted to increase faster than the supply, alternative production routes are sought for. Metathesis of ethene and 2-butene is an attractive alternative route to produce propene because it uses relatively cheap and abundant olefins to produce another more valuable olefin. First exploited by Phillips in the so-called “Phillips Triolefin Process” [2], the metathesis of light alkenes is now an important industrial process for the production of propene [3].

The most successful heterogeneous catalysts are based on supported W [4–7], Mo [8–10] and Re [11–14] oxides. Among them,

tungsten-based catalysts are attractive because they are tolerant towards the impurities found in the industrial feed streams (thus affording long lifetime) [15,16]. Various supports have been studied, including alumina [17,18], silica [7,19,20], silica-alumina [4,19], silica-titania [21,22] and mesoporous molecular sieves [23]. It must be noticed that excellent performance was recently demonstrated with alumina supported tungsten hydride catalysts [24,25].

The molecular structure of supported tungsten oxide is obviously dependent on the nature of the support [26]. It has been confirmed that crystalline WO₃ is not active for metathesis [27–29]. Only amorphous tungsten oxide species exhibit metathesis activity and it has been shown that high dispersion is a prerequisite for high activity [4,17]. WO₃/SiO₂ is known to be active and stable at relatively high temperature (300–500 °C). It is not possible to boost further the activity at higher temperature, for isomerization and cracking reactions would also be further favoured [30]. Silica is a barely acidic support, so the interactions between WO_x surface species and silica are weak and lead to the formation of condensed species that are inactive. Alumina supports exhibit strong acid sites which can promote the dispersion of WO_x surface species but also lead to too higher isomerization activity and thus poor metathesis

* Corresponding author. Tel.: +32 10473648.

E-mail address: damien.debecker@uclouvain.be (D.P. Debecker).

performance. Accordingly, mixed silica-alumina supports have been investigated in a search for better dispersion, reducibility, acidity [4,31]. In the present study, both silica and silica-alumina supported systems will be studied.

Classically, WO_3 -based catalysts are prepared by impregnation methods [32]. A support is prepared first, and then a W precursor is deposited by impregnation. The solvent is then eliminated by filtration or evaporation and the catalyst is dried and calcined. This multi-step method can present several limitations: inhomogeneity of the deposit, pore plugging, genesis of inactive species (crystals), etc. Even if metathesis activity can be improved by controlling activation procedure or reaction conditions (e.g. composition and purity of the olefin feed) it is now undeniable that the catalyst preparation itself is responsible for most of the performance limitations [5,8]. Therefore more innovative routes are being investigated with the aim to better control the formation of tungsten surface species and in turn to improve the intrinsic activity of the catalysts [6,31].

Sol-gel chemistry is a powerful tool for the design of oxides and mixed oxides [33,34]. However, the preparation of elaborate catalysts involving an active oxide phase dispersed at the surface of a mixed oxide support remains a challenge. While conventional hydrolytic sol-gel routes [35] often require complicated procedures (multi-step methods, precursor reactivity modification, supercritical drying, use of a templating agent, etc.) non-hydrolytic routes [36] have recently emerged as a decisive method for catalyst preparation. A recent review [37] describes the different non-hydrolytic routes in details and presents a comprehensive overview of the different kind of catalysts that can be prepared: mixed oxides, crystalline nanoparticles, single site catalysts, etc.

Non-hydrolytic routes based on the reaction of chloride precursors with alkoxide precursors or diisopropyl ether were shown to provide an excellent control over the stoichiometry and the homogeneity of mixed oxide gels [38]. Owing to the generally high degree of condensation of non-hydrolytic gels, mesoporous xerogels with high surface area and pore volume can be obtained by simple evaporative drying and without templating agent. Accordingly, these nonhydrolytic routes are attracting increasing attention for the preparation of mixed oxide catalysts [39–45]. This route has been proposed for the preparation of Mo- and Re-based metathesis catalysts [13,46–48]. In general the metathesis catalysts prepared by NHSG exhibited high surface area, large pore volume, large mesopores, and high dispersion of the active oxide. Nevertheless, Mo- and Re-based catalysts – either made by impregnation of NHSG – tend to suffer from relatively fast deactivation.

In the present paper we describe the first one-step NHSG preparation of the industrially relevant $\text{WO}_3\text{-SiO}_2$ metathesis catalysts. The WO_3 loading is varied in a systematic way. We also turn our attention toward ternary $\text{WO}_3\text{-SiO}_2\text{-Al}_2\text{O}_3$ formulation, assessing the effect of alumina addition. The new catalysts were tested in the cross-metathesis of ethene and *trans*-2-butene and they were characterized by N_2 -physisorption, XRD, NH_3 -TPD, NH_3 -chemisorption, Raman spectroscopy, XPS, TPR and ICP-AES. Two catalysts prepared by incipient wetness impregnation of commercial silica and silica-alumina supports are used as benchmarks.

2. Experiments

2.1. Preparation of the catalysts

The non-hydrolytic sol-gel syntheses [37] were performed under an argon atmosphere using a glove box. SiCl_4 (Alfa Aesar, 99.9%), AlCl_3 (Alfa Aesar, 99.9%), and WCl_6 (Alfa Aesar, 99.5%) were used as received. Diisopropyl ether ($^i\text{Pr}_2\text{O}$) was purchased from Aldrich with 99% purity and was further dried by distillation over

a sodium wire. The catalysts were prepared in 80 ml autoclaves as to obtain 2 g of mixed oxide. The catalysts were prepared by reaction of the chloride precursors with a stoichiometric amount of $^i\text{Pr}_2\text{O}$: the number of moles of $^i\text{Pr}_2\text{O}$ was calculated so that the number of ^iPr groups in $^i\text{Pr}_2\text{O}$ was equal to the total number of Cl groups in the precursors. The requested quantity of chloride precursors were introduced first in the autoclave, then $^i\text{Pr}_2\text{O}$ was added. Finally, the solvent (20 ml of CH_2Cl_2) was introduced. The solution obtained was heated at 110 °C for 4 days under autogeneous pressure (ca. 0.7 MPa). After cooling down to room temperature, the gel was washed with CH_2Cl_2 3 times (75 ml) and dried at 20 °C under vacuum (10 Pa) for 1 h and then at 120 °C for 4 h. The xerogel was then crushed in a mortar and calcined in a muffle oven for 5 h at 500 °C (heating rate 10 °C/min). The catalysts are labelled “ $x\text{WSi}$ ” or “ $x\text{WSiAl}$ ” where x represents the nominal WO_3 loading (wt.%) and y is the nominal Al_2O_3 loading (wt.%).

The reference catalysts were prepared by an incipient wetness impregnation method (IW) using an aqueous solution of ammonium metatungstate hydrate (99.9%, Aldrich) as the tungsten precursor. The nominal WO_3 loading was 10 wt.%. Commercial SiO_2 (99.9% grade 646, Aldrich) and $\text{SiO}_2\text{-Al}_2\text{O}_3$ (99.9% grade 135, 13 wt.% alumina, Aldrich) were employed as catalyst supports. After impregnation, the catalysts were dried at 110 °C overnight followed by calcination. These samples are labelled 10W-Imp-Si and 10W-Imp-SiAl.

2.2. Characterization of the catalysts

The weight percentages of W, Si, and Al were measured by inductively coupled plasma-atomic emission spectroscopy (ICP-AES) on a ICP AES 6500 from Thermo Scientific. The materials were dried at 378 K prior to measurements.

N_2 physisorption measurements were performed at -196 °C on a Micromeritics Tristar. The samples were outgassed at 150 °C under vacuum (5 Pa) overnight. Specific surface area (S_{BET}) was determined by the BET method. Mean pore size was derived by using the formula $4V_p/S_{\text{BET}}$.

Powder X-ray diffraction (XRD) diffractograms of all catalysts were obtained with a SIEMENS D5000 X-ray diffractometer using $\text{CuK}\alpha$ radiation in the 2θ range of 5–75 degrees.

NH_3 -temperature programmed desorption (TPD) and NH_3 -chemisorption were used to characterize the surface acidity. Ammonia chemisorption on fresh catalysts was determined volumetrically using the Micromeritics ASAP2010 Chem apparatus, as described in details elsewhere [49]. Briefly, in a typical experiment, 100 mg of the catalyst was placed in a U-shaped sample tube, flushed under a He flow at 300 °C for 2 h and then evacuated at 50 °C for 2 h down to a residual pressure lower than 0.66 Pa. The first NH_3 adsorption isotherm was measured at 50 °C. Then the sample was evacuated at the same temperature and down to <0.66 Pa again. Subsequently, a second NH_3 adsorption isotherm was taken. The difference between the two isotherms represents the amount of NH_3 still chemisorbed on the sample after evacuation at 50 °C and under vacuum (<0.66 Pa). Expressed in terms of cm^3 of chemisorbed NH_3 per gram of catalyst, this value is then normalized by the specific surface area of the sample, to give its “total surface acidity”. The same experiment is carried out a second time (on a fresh sample), also taking the two consecutive isotherms at 50 °C but the intermediate evacuation down to <0.66 Pa pressure is run at 150 °C. The difference between the two isotherms gives the amount of NH_3 still chemisorbed on the sample after evacuation at 150 °C and under vacuum, which is also normalized by the specific surface area to give the “strong surface acidity” of the sample. The standard deviation for each reported value is lower than 10% in relative.

NH₃-TPD measurements were carried out in a quartz reactor on a Hiden Analytical Catlab-PCS. The sample (100 mg) was preheated in helium at 300 °C for 60 min with heating rate of 10 °C/min. NH₃ adsorption was done at 50 °C in a 5% NH₃/He (20 ml/min) for 30 min. Physisorbed NH₃ was removed by purging with helium at 50 °C for 40 min (50 ml/min). Chemisorbed NH₃ was then desorbed by heating the sample from 50 to 600 °C with ramping rate of 15 °C/min, to yield the TPD profile (NH₃ signal detected at the MS).

Temperature programmed reduction (TPR) under H₂ was carried out in the same apparatus. Prior to these measurements, the sample is pretreated with a N₂ flow for 1 h at 500 °C (50 ml/min), and then cooled down to 50 °C in a N₂ flow (50 ml/min). A 5% H₂/N₂ flow (40 ml/min) was then admitted through the reactor and the catalyst was heated from 50 to 950 °C with a heating rate of 10 °C/min. The H₂ consumption and the water production were measured by MS.

X-ray photoelectron spectroscopy (XPS) was performed on a SSI-X-probe (SSX-100/206) spectrometer equipped with a monochromatized microfocused Al K α X-ray source, operating at 10 kV and 12 mA. After outgassing under vacuum (10⁻³ Pa) overnight, the samples were placed in the analysis chamber where the residual pressure was of about 10⁻⁵ Pa. The charging effects were compensated using a flood gun energy at 8 eV and a fine-meshed nickel grid placed 3 mm above the sample surface. The pass energy was 150 eV and the spot size was 1000 μm , leading to an energy resolution of 1.6 eV. The angle between the normal to the sample surface and the direction of electron collection was 55°. All the binding energies were referenced to the Si 2p peak at 103.5 eV. The following sequence of spectra was recorded: survey spectrum, C 1s, O 1s, Si 2p, Al 2p, W 4d, Cl 2p and C1s again to check for charge stability as a function of time and for the absence of degradation of the sample during the analyses. The binding energy (BE) values were referred to the Si 2p peak fixed at 103.4 eV as recommended for samples with changing composition [50].

Raman spectra were recorded at room temperature on a Thermo Scientifi DXR Raman microscope using the 780 nm laser with 14 mW power. The resolution was 4 cm⁻¹. Acquisition time was 10 s, and 100 scans were recorded and averaged for each sample.

2.3. Cross-metathesis reaction

The catalyst (1 g) was placed at the centre of stainless steel tubular reactor having an inner diameter (ID) of 7.5 mm and mounted with a type K thermocouple. It was then pretreated at temperature not greater than 600 °C under nitrogen flow for 1 h and cooled down to the reaction temperature of 450 °C before the reactant feed was admitted. The reactant feed consisted in the mixture of 2% *trans*-2-butene and 4% ethene balanced with N₂. The reaction conditions were as follows: pressure = 0.1 MPa, the total flow rate

was 20 cm³ min⁻¹, and 10 h on stream. The composition of products and feed stream were analyzed by a Shimadzu GC-2014 gas chromatograph equipped with a column of packed 10% silicone SE-30 (3.02 m with 0.53 mm ID) and a flame ionization detector using nitrogen as the carrier gas (5 ml/min).

The conversion of *trans*-2-butene (Eq. 1), the propene selectivity (Eq. 2) and the propene yield (Eq. 3) are calculated using the following equations:

$$\text{Trans-2-butene conversion}(\%)$$

$$= 100 \times \frac{(\text{mol trans-2-butene}_{\text{IN}} - \text{mol trans-2-butene}_{\text{OUT}})}{\text{mol trans-2-butene}_{\text{IN}}} \quad (1)$$

$$\text{Propene selectivity}(\%) = 100 \times \frac{\text{mol propene}_{\text{OUT}}}{\text{mol total products}_{\text{OUT}}} \quad (2)$$

$$\text{Propene yield}(\%) = \text{trans-2-butene conversion}$$

$$\times \text{propene selectivity} \quad (3)$$

The catalytic test was duplicated on 10W-Imp-Si catalyst and the experimental variation was below 1% and below 5% for conversion and selectivity, respectively.

3. Results and discussion

3.1. Composition, texture and crystallinity

Four binary formulations (WO₃-SiO₂) were prepared with 5, 10, 15 or 20 wt.% of WO₃ in nominal. Similarly, four ternary formulations (WO₃-SiO₂-Al₂O₃) were prepared with 10 wt.% of WO₃ and 5, 10, 15 or 20 wt.% of Al₂O₃ in nominal. The tungsten and aluminium contents have been checked by ICP-AES. Table 1 shows that experimental weight content corresponds well to theoretical content and thus that NHSG provides a good control over the final composition of the mixed oxides.

Analysis of their texture shows that all samples were mesoporous, with N₂ adsorption-desorption isotherms of type IV (Fig. 1). The sol-gel samples had specific surface areas ranging between 560 to 750 m² g⁻¹ and average pore diameters ranging between 3.5 and 9.9 nm depending on the composition (Table 1). The texture of binary WO₃-SiO₂ catalysts was not markedly affected by changing the WO₃ loading, even if a slight increase in average pore diameter is observed with increasing WO₃ loading. Pore diameter and pore volume were larger in the silica-alumina-based catalysts. At high alumina content, the specific surface area decreases slightly. Briefly said, all NHSG samples exhibit a mesoporous texture with large specific surface area, pore diameter and pore volume.

Table 1
WO₃ loading measured by ICP-AES and textural properties of the studied samples.

Catalysts	WO ₃ (wt %) ^a	Al ₂ O ₃ (wt %) ^a	S _{BET} (m ² g ⁻¹)	V _P (cm ³ g ⁻¹)	D _P (nm)
Silica	–	–	290	1.2	11.5
Silica-Alumina	–	nm	480	0.7	5.9
5WSi	5.1	–	750	0.7	3.5
10WSi	10.9	–	750	0.8	4.2
15WSi	17.5	–	780	1.0	5.2
20WSi	19.1	–	680	1.0	5.7
10WSi5Al	10.3	5.4	710	1.3	7.2
10WSi10Al	8.6	10.5	740	1.7	9.0
10WSi15Al	10.0	15.5	570	1.4	9.9
10WSi20Al	9.1	20.8	580	1.3	8.8
10W-Imp-Si	10.7	–	250	0.8	13.1
10W-Imp-SiAl	10.9	11.2	370	0.5	5.8

^a The WO₃ and Al₂O₃ loading is calculated on the basis of the W and Al content, considering that W and Al are fully oxidized and thus present in the form of WO₃ or Al₂O₃ respectively. "nm" stands for "not measured".

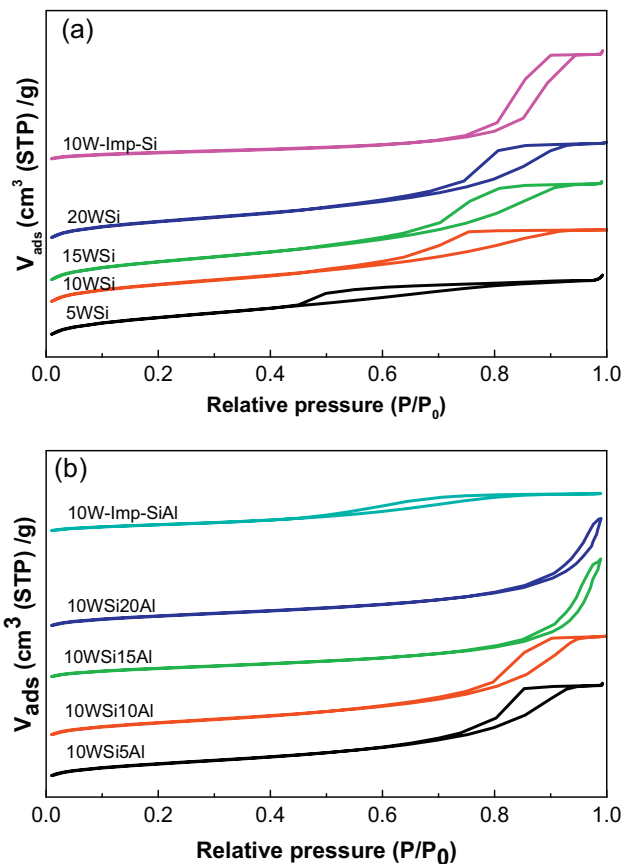


Fig. 1. N₂-physisorption isotherms (adsorption and desorption) measured on (a) the catalysts with binary composition, (b) the catalysts with ternary composition. Curves have been shifted along the y-axis for the sake of clarity.

Both commercial supports (silica and silica-alumina) are also mesoporous but exhibit slightly lower surface areas. Understandably, the specific surface area and pore volume decreased after impregnation, especially for the silica-alumina. The average pore size and pore size distribution (see Fig. S1) remained almost unchanged. It suggests that WO₃ is mainly deposited at the outer surface of the support particles (not in the pores). It should be noted that more advanced impregnation techniques (use of peroxy precursors, functionalization of the silica surface, etc.) can be implemented to get better W dispersion.

X-ray diffraction analysis of the different sol-gel samples are shown in Fig. 2. NHSG catalysts all exhibited the broad band around

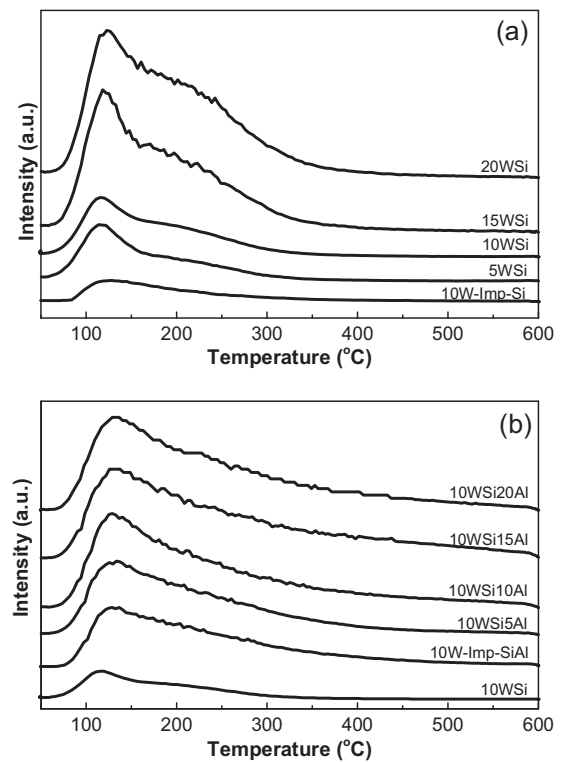


Fig. 3. NH₃-TPD profiles of supported tungsten oxide catalysts. Curves have been shifted along the y-axis for the sake of clarity.

20–25° attributable to the amorphous solids. For binary WO₃-SiO₂ samples, small peaks of WO₃ crystals (23.12°, 23.60° and 24.38°) are detected from 10 wt.% loading and their intensity tends to increase with the WO₃ loading. In contrast intense diffraction lines of WO₃ are detected in the samples prepared by incipient wetness impregnation. There was no evidence of WO₃ crystals in the patterns of the Al-containing samples, thus confirming that W oxide tends to be better dispersed in/on silica-alumina matrix as compared to silica. For completeness of the description, Raman spectroscopy was applied and confirmed the presence of crystalline species in the impregnated catalysts and of more dispersed species in NHSG catalysts (see supplementary information, Fig. S2).

3.2. Surface chemistry and reactivity

Temperature programmed desorption of ammonia (NH₃-TPD) was used to probe the acidity of the catalysts (Fig. 3). The acidity of the sol-gel samples strongly depends on their composition. Since silica support is barely acidic, the acidity in binary WO₃-SiO₂ catalysts mainly originates from the presence of the tungsten oxide [51]. As proposed by Katada et al. we consider that the main peak centred at 110–130°C can be attributed to weak acid sites and that higher temperature desorption can be attributed to medium and strong acid sites [52]. More precise identification of desorption peaks is too delicate as the desorption profile indicates that a family of acid sites with various strength is usually present. In the binary WO₃-SiO₂ catalysts acidity clearly increases with the WO₃ loading. Ammonia desorption stops around 320°C. Acidity is clearly higher and stronger in all ternary WO₃-SiO₂-Al₂O₃ catalysts, exhibiting a more intense desorption peak with a tail up to relatively high temperature (~500°C).

The acidity of the catalysts was also analysed by NH₃-chemisorption to confirm NH₃-TPD results and obtain more quantitative data (Fig. 4). Strong and weak acidic sites are defined arbitrarily as explained in the experimental part. The results are

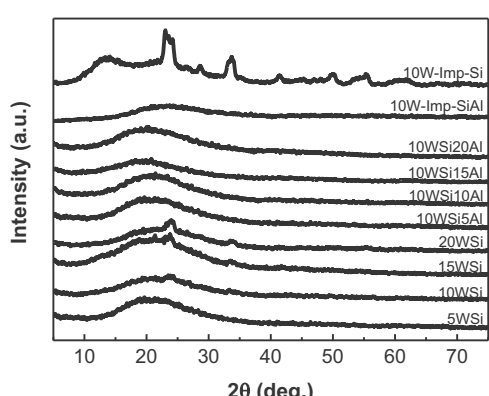


Fig. 2. XRD patterns of supported tungsten oxide catalysts. Diffractograms have been shifted along the y-axis for the sake of clarity.

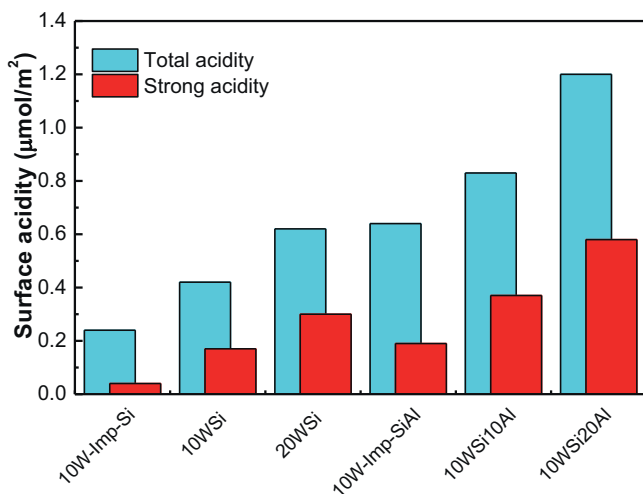


Fig. 4. Acidity (acid site density) of impregnated and sol-gel catalysts measured by NH₃-chemisorption. The total acidity (amount of chemisorbed NH₃ per square meter of sample after desorption at 50 °C) is represented by the blue columns and the strong acidity (amount of chemisorbed NH₃ per square meter of sample after desorption at 150 °C) is given in the red columns. The difference between both columns represented the weak acidity. Acidity is normalized by the surface area.

expressed in moles of NH₃ adsorbed per m² (acid site density). The silica-supported catalyst prepared by impregnation is confirmed to be only weakly acidic with virtually no strong acid sites. The corresponding 10WSi catalyst prepared by NHSG is however significantly more acidic and exhibits a significant proportion of strong acid sites. While the composition is matching, acidity is clearly different and this can be attributed to the fact that WO_x surface species are dispersed in the silica matrix and only marginally form WO₃ crystals in the NHSG catalyst. If the WO₃ loading is further increased to 20%, acidity further increases (both total and strong). So even if the amount of WO₃ crystals increases with the loading, it is clear that dispersed and acidic WO_x surface species are also building up. The total acidity of the silica-alumina-supported catalyst prepared by impregnation is about three times higher than that of the silica supported one. About one third of the acid sites can be ranked in the “strong” category. Again, NHSG made catalysts present higher amount of total and strong acid sites. This can be taken as an indication of high dispersion and strong interaction between the W oxide species and the silica-alumina matrix.

H₂-TPR was used to investigate the reducibility of tungsten species (Fig. 5). This provides indications on the nature of the interaction with the support or matrix. The reduction of pure WO₃

Table 2

Surface characterization by X-ray photoelectron spectroscopy (XPS) on the references catalysts and on the NHSG catalysts before calcination (xerogels, marked with a “X”) and after calcination.

Catalysts	Si (at %)	O (at %)	C (at %)	Cl (at %)	Al (at %)	W (at %)
10W-Imp-Si	35.5	62.9	1.4	–	–	0.22
10W-Imp-SiAl	27.5	60.2	7.3	–	–	0.40
5WSi-X	29.1	62.7	7.2	0.8	–	0.21
5WSi	31.3	65.9	2.6	–	–	0.25
10WSi-X	27.7	57.4	9.5	4.9	–	0.54
10WSi	32.3	63.9	3.3	–	–	0.55
15WSi-X	26.5	61.1	9.9	1.3	–	1.13
15WSi	29.5	62.5	7.0	–	–	0.99
20WSi-X	25.5	60.5	10.3	2.0	–	1.76
20WSi	28.8	64.4	5.8	–	–	0.94
10WSi5Al-X	26.6	54.3	14.8	2.2	1.6	0.54
10WSi5Al	28.4	59.4	9.8	–	1.8	0.55
10WSi10A-X	21.4	51.4	21.3	1.7	3.6	0.65
10WSi10Al	26.1	60.5	8.1	–	4.5	0.67
10WSi15Al-X	20.0	55.4	18.5	1.5	4.2	0.43
10WSi15Al	25.2	61.9	7.6	–	4.8	0.44
10WSi20Al-X	18.1	50.9	22.2	2.0	6.3	0.45
10WSi20Al	23.9	60.9	7.8	–	7.0	0.50

exhibited three peaks with maxima at 665 °C, 755 °C and 950 °C. WO₃ in 10W-Imp-Si is mainly reduced at 790 °C. This is a classical result for silica-supported WO₃ crystals [53]. It correlates with XRD and indicates that the interactions with the support are weak. In the corresponding NHSG samples no reduction is observed in the whole range of temperature explored indicating that the amount of WO₃ accessible to H₂ (at the surface) is much lower and that the reducibility is very low, due to a more intimate interaction with the silica matrix. Only at 20 wt.% WO₃ loading (20WSi) a small reduction event was detected at 685 °C. This also correlates well with the onset of small WO₃ crystals seen in XRD. The Si-Al containing catalysts (prepared by either the impregnation or the sol gel) present no clear reduction event, indicating that they were hardly reducible.

The surface composition of all catalysts was investigated by XPS (Table 2). Xerogels (i.e. the mixed oxide recovered after non-hydrolytic sol-gel polycondensation but before calcination) were also analyzed. As expected, the Cl and C content was high in xerogels. After calcination however, Cl contamination was eliminated and C contamination dropped to a level usually seen in XPS with clean samples. Logically, W surface concentration increased with the bulk nominal WO₃ loading. The same holds for alumina. It can be noted that for similar Mo- and Re-based catalysts, a migration of the active oxide toward the catalyst surface was observed [13,47], provoked by the calcination step. This was explained by the limited solubility of Mo and Re oxides in the silica(-alumina) matrix and by their low Tamman temperature. In the present case no W enrichment of the catalyst surface is observed. Tungsten oxide indeed has a relatively high Tamman temperature (600 °C) and has thus limited mobility in the silica(-alumina) matrix under the calcination temperature applied here (500 °C). On the contrary, at high WO₃ loading, the surface W concentration drops after calcination. This may tentatively be correlated with the formation of some small WO₃ crystals during calcination at the expense of dispersed surface species. Interestingly, the Al content seems to have an impact on the W dispersion in the ternary mixed oxides with fixed WO₃ loading and variable Al₂O₃ content. A maximum of W dispersion is obtained for the catalysts with 10 wt.% Al₂O₃ (10WSi10Al). Reference impregnation catalysts exhibit lower W surface concentration as compared to the corresponding NHSG samples, suggesting again that NHSG offers better W dispersion.

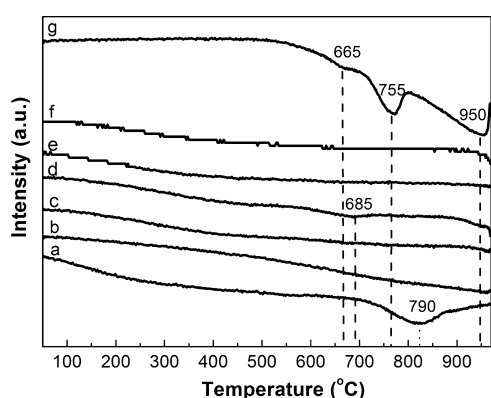


Fig. 5. H₂-TPR profiles of supported tungsten oxide metathesis catalysts. (a) 10W-Imp-Si; (b) 10W-Imp-SiAl; (c) 10WSi; (d) 20WSi; (e) 10WSi10Al; (f) 10WSi20Al; (g) WO₃. Curves have been shifted along the y-axis for the sake of clarity.

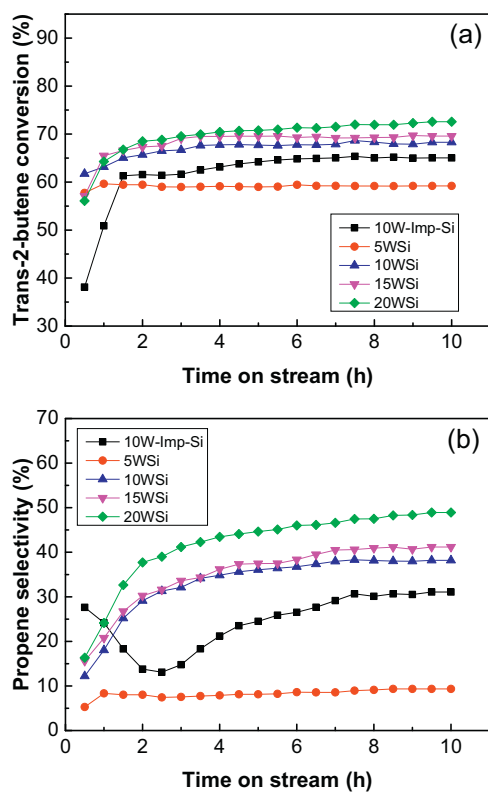


Fig. 6. Conversion of *trans*-2-butene (a) and propene selectivity (b) as a function of time-on-stream over binary $\text{WO}_3\text{-SiO}_2$ catalysts.

3.3. Metathesis activity and selectivity

All catalysts were tested in the cross-metathesis of *trans*-2-butene and ethene at 450 °C. Catalytic activity as a function of time-on-stream is shown in Fig. 6 and Fig. 7 for binary and ternary formulations respectively. Note that selectivity is here calculated considering *cis*-2-butene as a product even though it can still react with ethene to yield propene. The 10W-Imp-Si catalyst – that mimics the industrial catalyst – allows converting 60–65% of *trans*-2-butene (Fig. 6). However, the selectivity for propene is not stable over time, fluctuating between 10 and 30% and finally reaching about 30% after 8 h of reaction. This corresponds to approximately 20% propene yield (Table 3).

The corresponding NHSG sample with the same WO_3 loading performs significantly better, exhibiting both higher conversion and higher selectivity. The yield is stabilized at 26% after 8 h. The metathesis activity increased with increasing tungsten loading. While the sample with only 5 wt.% WO_3 shows poor performance, increasing the loading to 15 or 20 wt.% allows achieving 28 or 34% propene yield, respectively.

Addition of Al oxide in these NHSG catalysts has a dramatic impact on the catalytic performance (Fig. 7). Conversion readily reaches about 90% for all catalysts, without induction period. Selectivity ranges between 35 and 60% depending on the alumina content. As found earlier for MoO_3 -based catalysts [48,49], an intermediate alumina content of 10 wt.% is the most appropriate. This catalyst achieves 55% propene yield, significantly outcompeting the corresponding catalyst prepared by impregnation (35%).

3.4. Correlating performance and properties

The fact that one-pot sol-gel catalysts perform better than corresponding impregnated catalysts (both in the binary and ternary systems) can tentatively be attributed to the higher acidity

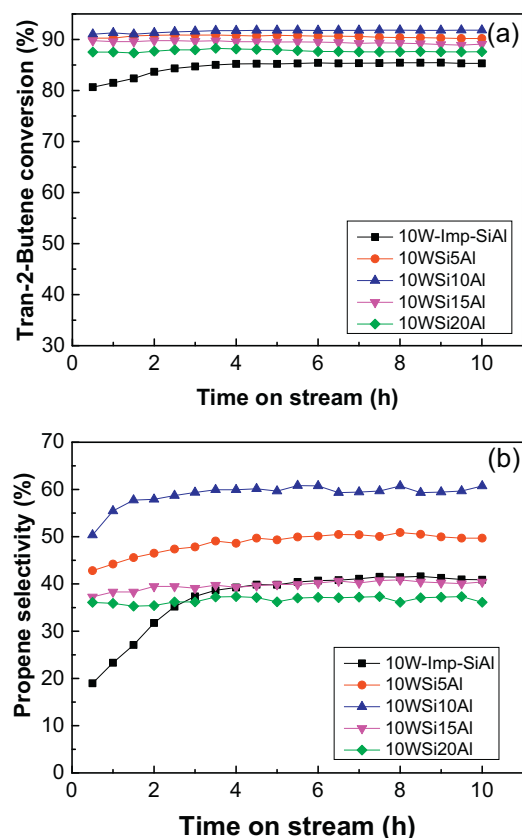


Fig. 7. Conversion of *trans*-2-butene (a) and the propene selectivity (b) as a function of time-on-stream over ternary $\text{WO}_3\text{-SiO}_2\text{-Al}_2\text{O}_3$ catalysts.

exhibited by the former catalysts, as well as their lower reducibility and their higher specific surface area.

The mechanism of the metathesis reaction starts from the in-situ formation of W-carbenes by reaction of the WO_x surface species with the olefins present in the feed [54]. It is known that well dispersed tetrahedral tungsten species react better to yield the desired carbene species, as compared to condensed forms of tungsten oxide (polymeric surface species, WO_3 crystals) [2,16,55]. Dispersed WO_x species also tend to be less reducible and more acidic. According to XRD (Fig. 2), WO_3 crystallites were clearly observed on impregnated silica catalyst while the corresponding NHSG catalysts remained mostly amorphous (weak diffraction lines observed only at high WO_3 loading). XPS also indicate better surface dispersion. It should be noted however that this is not necessarily an indication for isolated WO_x species and that oligo- or polymeric species can be expected too. Previous study on MoO_3 -based metathesis catalysts has demonstrated that oligomeric species can be present already at very low loading [56]. The better dispersion of tungsten oxide is a clear advantage of NHSG catalysts over impregnated ones. Interestingly, sol-gel catalysts also reached equilibrium activity faster.

It must be recalled that sol-gel techniques present the downside of dispersing the active elements also in the bulk of the material, thus not accessible for the surface reaction. Fortunately, the binary $\text{WO}_3\text{-SiO}_2$ catalysts presented here exhibited high specific surface area, thereby minimizing pore wall thickness and maximizing the proportion of W surface species. XPS also confirmed that the dispersion of W at the surface of these NHSG catalysts was high. No WO_3 crystal was detected in alumina-containing catalysts, either made by impregnation or NHSG. Nevertheless, most NHSG catalysts performed better than the impregnated catalyst. NHSG catalysts showed much higher specific surface area. Interestingly, the alumina content has a consistent effect on texture,

Table 3

Conversion, selectivity and propene yield for each catalyst. Values are an average of the experimental values obtained between 8 and 10 h on stream.

Catalysts	Trans-2-butene conversion (%)	Selectivity					Propene yield (%)
		Propene	1-Butene	Cis-2-butene	Others ^a	iso-Butene	
10W-Imp-Si	65	31	33	34	2.1	–	20
5WSi	59	9	43	48	0.4	–	5.5
10WSi	68	38	28	30	3.2	–	26
15WSi	69	41	27	29	2.9	–	28
20WSi	72	48	24	24	3.5	–	34
10W-Imp-SiAl	85	41	39	12	6.2	1.3	35
10WSi5Al	90	50	26	8	11	4.9	45
10WSi10Al	92	60	20	6	11	3.1	55
10WSi15Al	89	40	30	9	15	5.3	36
10WSi20Al	88	37	34	10	14	4.5	32

^a 1-pentene, cis-2-pentene, trans-2-pentene, 1-hexene (C_5 and C_5^+).

W surface concentration measured by XPS and metathesis activity. The formulations that exhibit lower surface area and lower W surface concentration yielded lower metathesis activity. They also showed poorer selectivity to propene and higher selectivity for side isomerization reactions catalysed by acidic sites [55]. This lack of selectivity can thus tentatively be correlated to an excessive acidity on these formulations. On the contrary, the catalyst with 10 wt.% Al_2O_3 had the highest specific surface area, the highest W surface concentration and the highest propene yield.

4. Conclusions

A new one-pot preparation route based on non-hydrolytic sol-gel is presented as a powerful new method to prepare highly active WO_3 - SiO_2 and WO_3 - SiO_2 - Al_2O_3 metathesis catalysts. These new catalysts reach high propene yields in the industrially relevant metathesis conditions, as they clearly outcompete the classical catalysts prepared by incipient wetness impregnation. The method offers a good control on the final catalyst composition and provides mixed oxides with excellent textures (large mesopores, high surface area). It uses relatively cheap chloride precursors. Decisively, non-hydrolytic sol-gel catalysts feature high W dispersion, which correlates with lower reducibility, higher acidity and higher metathesis activity. Activity is governed by the catalyst composition. Increasing the WO_3 loading in the binary WO_3 - SiO_2 formulations leads to higher activity. Further addition of alumina is beneficial too, but an optimum is found at 10 wt.% Al_2O_3 . While Al_2O_3 addition seems to contribute to the better dispersion of tungsten oxide, it also appears to favour side reactions towards 1-butene, cis-2-butene and iso-butene.

Acknowledgements

The authors thank Dr. P.H. Mutin and Dr. K. Bouchmella for all the precious advices and help on the NHSG method. J.-F. Gousembourger is acknowledged for his work during an internship at IMCN.

Appendix A. Supplementary data

Supplementary data associated with this article can be found, in the online version, at <http://dx.doi.org/10.1016/j.apcata.2014.09.030>.

References

- [1] T. Ren, M. Patel, K. Blok, Energy 31 (2006) 425–451.
- [2] J.C. Mol, J. Mol. Catal. A 213 (2004) 39–45.
- [3] H. Fritz, (2008).
- [4] N. Liu, S. Ding, Y. Cui, N. Xue, L. Peng, X. Guo, W. Ding, Chem. Eng. Res. Des 91 (2013) 573–580.
- [5] S. Chaemchuen, S. Phatanasri, F. Verpoort, N. Sae-ma, K. Suriye, Kinet. Catal. 53 (2012) 247–252.
- [6] H.J. Liu, S.J. Huang, L. Zhang, S.L. Liu, W.J. Xin, L.Y. Xu, Catal. Commun. 10 (2009) 544–548.
- [7] S. Maksasithorn, D.P. Debecker, P. Praserthdam, J. Panpranot, K. Suriye, S.K.N. Ayudhya, Chin. J. Catal. 35 (2014) 232–241.
- [8] D.P. Debecker, M. Stoyanova, U. Rodemerck, E.M. Gaigneaux, J. Mol. Catal. A: Chem. 340 (2011) 65–76.
- [9] D.P. Debecker, M. Stoyanova, F. Colbeau-Justin, U. Rodemerck, C. Boissière, E.M. Gaigneaux, C. Sanchez, Angew. Chem. Int. Ed. 51 (2012) 2129–2131.
- [10] J. Handzlik, J. Stoch, J. Ogonowski, M. Mikolajczyk, J. Mol. Catal. A 157 (2000) 237–243.
- [11] W. Phongsawat, B. Netiworaruksa, K. Suriye, P. Praserthdam, J. Panpranot, J. Ind. Eng. Chem. 20 (2014) 145–152.
- [12] W. Phongsawat, B. Netiworaruksa, K. Suriye, S. Dokjampa, P. Praserthdam, J. Panpranot, J. Nat. Gas Chem. 21 (2012) 158–164.
- [13] K. Bouchmella, P. Hubert Mutin, M. Stoyanova, C. Poleunis, P. Eloy, U. Rodemerck, E.M. Gaigneaux, D.P. Debecker, J. Catal. 301 (2013) 233–241.
- [14] M. Stoyanova, U. Rodemerck, U. Bentrup, U. Dingderissen, D. Linke, R.W. Mayer, H.G.J. Lansink Rotgerink, T. Tacke, Appl. Catal. A 340 (2008) 242–249.
- [15] R.L. Banks, D.S. Banaslak, P.S. Hudson, J.R. Norell, J. Mol. Catal. 15 (1982) 21–33.
- [16] L.F. Heckelsberg, R.L. Banks, G.C. Bailey, Ind. Eng. Chem. Prod. Res. Dev. 7 (1968) 29–31.
- [17] R. Thomas, J.A. Moulijn, V.H.J. De Beer, J. Medema, J. Mol. Catal. 8 (1980) 161–174.
- [18] W. Grüner, W. Mörike, R. Feldhaus, K. Anders, J. Catal. 117 (1989) 485–494.
- [19] A. Andreini, J.C. Mol, J. Colloid Interface Sci. 84 (1981) 57–65.
- [20] Q. Zhao, S.L. Chen, J. Gao, C. Xu, Transition Met. Chem. 34 (2009) 621–627.
- [21] S. Chaemchuen, W. Limsangkass, B. Netiworaraksa, S. Phatanasri, N. Sae-Ma, K. Suriye, Bulg. Chem. Commun. 44 (2012) 87–91.
- [22] W. Limsangkass, S. Phatanasri, P. Praserthdam, J. Panpranot, W. Jareewatchara, S. Na Ayudhya, K. Suriye, Catal. Lett. (2013) 1–7.
- [23] T.I. Bhuiyan, P. Arudra, M.N. Akhtar, A.M. Aitani, R.H. Abudawoud, M.A. Al-Yami, S.S. Al-Khattaf, Appl. Catal., A 467 (2013) 224–234.
- [24] K.C. Szeto, E. Mazoyer, N. Merle, S. Norsic, J.M. Basset, C.P. Nicholas, M. Taoufik, ACS Catal. 3 (2013) 2162–2168.
- [25] E. Mazoyer, K.C. Szeto, N. Merle, S. Norsic, O. Boyron, J.-M. Basset, M. Taoufik, C.P. Nicholas, J. Catal. 301 (2013) 1–7.
- [26] I.E. Wachs, T. Kim, E.I. Ross, Catal. Today 116 (2006) 162–168.
- [27] A. Spamer, T.I. Dube, D.J. Moodley, C. Van Schalkwyk, J.M. Botha, Appl. Catal., A 255 (2003) 153–167.
- [28] S. Huang, S. Liu, W. Xin, J. Bai, S. Xie, Q. Wang, L. Xu, J. Mol. Catal. A: Chem. 226 (2005) 61–68.
- [29] S. Huang, F. Chen, S. Liu, Q. Zhu, X. Zhu, W. Xin, Z. Feng, C. Li, Q. Wang, L. Xu, J. Mol. Catal. A: Chem. 267 (2007) 224–233.
- [30] D. Lokhat, M. Starzak, M. Stelmachowski, Appl. Catal., A 351 (2008) 137–147.
- [31] D.P. Debecker, M. Stoyanova, U. Rodemerck, F. Colbeau-Justin, C. Boissière, A. Chaumonnot, A. Bonduelle, C. Sanchez, Appl. Catal., A 470 (2014) 458–466.
- [32] M. Zheng, S.L. Chen, J.H. Zhang, Y. Liu, L. Sang, J. You, X.D. Wang, Petroleum Sci. 10 (2013) 112–119.
- [33] F. Zaera, Chem. Soc. Rev. 42 (2013) 2746–2762.
- [34] G. Frenzer, W.F. Maier, Ann. Rev. Mater. Res. 36, 2006, 281–331.
- [35] A. Baiker, J.-D. Grunwaldt, C.A. Mueller, L. Schmid, Chimia 52 (1998) 517–524.
- [36] P.H. Mutin, A. Vioux, Chem. Mater. 21 (2009) 582–596.
- [37] D.P. Debecker, P.H. Mutin, Chem. Soc. Rev. 41 (2012) 3624–3650.
- [38] D.P. Debecker, V. Hulea, P.H. Mutin, Appl. Catal., A 451 (2013) 192–206.
- [39] B.L. Caetano, L.A. Rocha, E. Molina, Z.N. Rocha, G. Ricci, P.S. Calefi, O.J. de Lima, C. Mello, E.J. Nassar, K.J. Ciuffi, Appl. Catal., A 311 (2006) 122–134.
- [40] O. Lorret, V. Lafond, P.H. Mutin, A. Vioux, Chem. Mater. 18 (2006) 4707–4709.
- [41] P. Moggi, M. Devillers, P. Ruiz, G. Predieri, D. Cauzzi, S. Morselli, O. Ligabue, Catal. Today 81 (2003) 77–85.
- [42] A.F. Popa, P.H. Mutin, A. Vioux, G. Delahay, B. Coq, Chem. Commun. (2004) 2214–2215.
- [43] D.P. Debecker, K. Bouchmella, R. Delaigle, P. Eloy, C. Poleunis, P. Bertrand, E.M. Gaigneaux, P.H. Mutin, Appl. Catal. B 94 (2010) 38–45.
- [44] D.P. Debecker, R. Delaigle, K. Bouchmella, P. Eloy, E.M. Gaigneaux, P.H. Mutin, Catal. Today 157 (2010) 125–130.

- [45] A.M. Cojocariu, P.H. Mutin, E. Dumitriu, F.o. Fajula, A. Vioux, V. Hulea, *Chem. Commun.* (2008) 5357–5359.
- [46] K. Bouchmella, M. Stoyanova, U. Rodemerck, D.P. Debecker, P.H. Mutin, *Catal. Commun.* 58 (2015) 183–186.
- [47] D.P. Debecker, K. Bouchmella, C. Poleunis, P. Eloy, P. Bertrand, E.M. Gaigneaux, P.H. Mutin, *Chem. Mater.* 21 (2009) 2817–2824.
- [48] D.P. Debecker, K. Bouchmella, M. Stoyanova, U. Rodemerck, E.M. Gaigneaux, P.H. Mutin, *Catal. Sci. Technol.* 2 (2012) 1157–1164.
- [49] D.P. Debecker, D. Hauwaert, M. Stoyanova, A. Barkschat, U. Rodemerck, E.M. Gaigneaux, *Appl. Catal. A* 391 (2011) 78–85.
- [50] M. Jacquemin, M.J. Genet, E.M. Gaigneaux, D.P. Debecker, *ChemPhysChem* 14 (2013) 3618–3626.
- [51] Y. Wang, Q. Chen, W. Yang, Z. Xie, W. Xu, D. Huang, *Appl. Catal., A* 250 (2003) 25–37.
- [52] N. Katada, H. Igii, J.H. Kim, M. Niwa, *J. Phys. Chem. B* 101 (1997) 5969–5977.
- [53] B. Hu, H. Liu, K. Tao, C. Xiong, S. Zhou, *J. Phys. Chem. C* 117 (2013) 26385–26395.
- [54] J.L. Herisson, Y. Chauvin, *Makromol. Chem.* 141 (1971) 161.
- [55] A.J. Van Roosmalen, J.C. Mol, *J. Catal.* 78 (1982) 17–23.
- [56] D.P. Debecker, B. Schimmoeller, M. Stoyanova, C. Poleunis, P. Bertrand, U. Rodemerck, E.M. Gaigneaux, *J. Catal.* 277 (2011) 154–163.